electronic reprint

Journal of
Synchrotron Radiation
ISSN 0909-0495

An X-ray diffractometer for accurate structural invariant phase determination

Sérgio L. Morelhão

An X-ray diffractometer for accurate structural invariant phase determination

Sérgio L. Morelhão

Instituto de Física, USP, CP 66318, 05315-970 São Paulo, SP, Brazil. E-mail: morelhao@if.usp.br

Instrumental advances and experimental procedures for determining invariant triplet phases by *three*-beam X-ray diffraction are presented. A simple X-ray diffractometer is described. It allows the exploitation of the natural linear polarization of synchrotron radiation for eliminating systematic errors in triplet-phase determination. Examples of data-collection procedures with the diffractometer for composing a polarization-dependent set of azimuthal scans are given as well as the suggestion of an analytical procedure for extracting accurate triplet phases.

Keywords: reflection phase determination; *three*-beam X-ray diffraction; linear polarization; single crystals.

1. Introduction

X-ray waves diffracted by crystals are proportional to the Fourier components of the periodic electronic density of the medium, named structure factors. They carry precise information on the scattering power and position of each atom in the unit cell. Since the intensity of an electromagnetic wave depends on the modulus square of its amplitude, the phases of the structure factors are not measurable by X-ray detectors. This is known as the crystallographic phase problem. The structure determination methods currently available are based on measurements of the structure factor modulus, combined with phasing procedures (see Helliwell, 2002, and references therein) that have allowed thousands of crystal structures to be known today. However, whatever the phasing procedure used, it is also based on intensity data collection of several reflections. The number of measured intensities and complexity of the structures limit the accuracy of the phase values assigned to each reflection. On this scenario, direct experimental measurements of reflection phases with good accuracy can provide alternative information about the crystalline structure without the necessity of refining the resolution of the whole structure.

Interference of the X-ray diffracted waves has been investigated for decades as a possible procedure for physically measuring reflection phases (Hart & Lang, 1961; Colella, 1974; Post, 1977; Shen & Colella, 1987; Chang, 1982; Weckert & Hümmer, 1997; Stetsko *et al.*, 2001, and many others). The simplest way to set two diffracted waves to interfere is by exciting a *three*-beam diffraction (*3*-BD) in a crystal. When it is excited, each diffracted beam is a sum of two wavefields, *i.e.* the $\mathbf{E}_P$ and $\mathbf{E}_S$ waves shown in Fig. 1. The primary wave $\mathbf{E}_P$ is produced by a single reflection (reflection A) while the secondary wave $\mathbf{E}_S$ comes from a double-bounce reflection formed by reflection B plus the coupling reflection C, whose indexes are given by $A - B$. By keeping one wave excited and changing the angular condition of the other, characteristic interference profiles are obtained. The most common is the interference profile obtained by an azimuthal scan (ϕ-scan) of the sample, where the intensity $I(\phi) = |\mathbf{E}_P + \mathbf{E}_S(\phi)|^2$ is a function of the crystal rotation around the diffraction vector, $\mathbf{g}_A$, of the reflection A. Since the primary wave is kept excited during the ϕ rotation, its strength is taken as constant in a first approximation (a correction to this approximation will be discussed later). Normalized by the intensity of the primary reflection $|\mathbf{E}_P|^2$, $I(\phi)$ can be written as

$$I_{\rm nor}(\phi) = 1 + R^2(\phi) + 2\xi R(\phi)\cos\gamma\cos(\Delta\psi). \quad (1)$$

It is very similar to the expression of any two interfering electromagnetic waves with a phase difference $\Delta\psi$, an amplitude ratio $R(\phi) = |\mathbf{E}_S(\phi)|/|\mathbf{E}_P|$, and an angle γ between the oscillation directions of the wavefields $\mathbf{E}_P$ and $\mathbf{E}_S$. For the moment $\xi = 1$, and the reason for including it is discussed below. The phase difference is the sum of two phase angles: the invariant phase triplet $\delta_T = \delta_B + \delta_C - \delta_A$ where δ_G is the phase of the structure factor of reflection G (= A, B or C), and the phase shift $\Omega(\phi)$ of the resonant term, the term that describes the excitation of the secondary wave due to the crystal rotation (Weckert & Hümmer, 1997). In other words, $\Delta\psi = \Omega(\phi) + \delta_T$, where $\Omega(\phi)$ is well known from X-ray diffraction theory and δ_T is the desired triplet-phase value to be determined from experiment.

Equation (1) represents the simplest available approach of the *3*-BD phenomenon, also known as the second-order Born approximation (Shen & Colella, 1988; Chang & Tang, 1988). In spite of its simplicity, after some modifications this theoretical approach has recently been used for measuring triplet-phase values from experimental ϕ-scans with very good accuracy (Morelhão & Kycia, 2002). The major modification in the approach consists of fitting the experimental profiles with an extra parameter ξ in equation (1), varying in the range from 0 to 1, *i.e.* $0 \le \xi \le 1$. The practical effect of this parameter is to reduce the contribution of the interference term of the azimuthal profiles. This can be understood as a loss of coherence of the diffracted beams or as if the diffracted beams would have a partial capability to interfere. However, further discussion on any physical justification of this parameter is beyond the scope of this article, which is just intended to present the equipment and measuring procedures used for accurate triplet-phase determination as well as to discuss its relevance.

In this article, a simple and low-cost X-ray diffractometer is described. It has been designed specially to explore the strength tuning of the multiple-diffracted waves by the linear polarization of

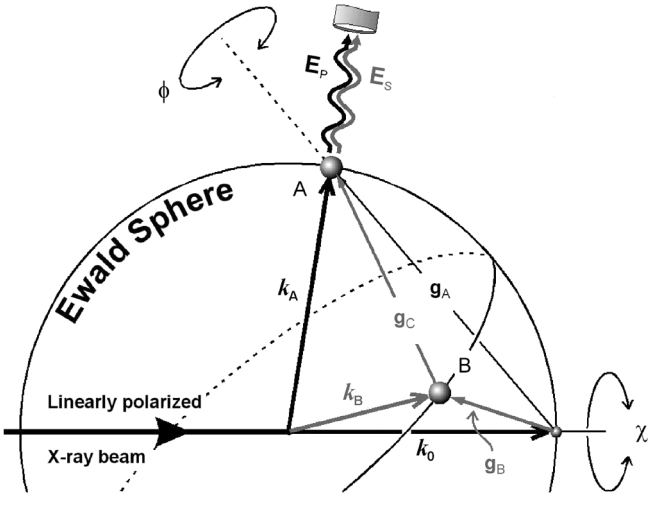

Figure 1
Ewald construction of a *three*-beam diffraction in reciprocal space. Wave $\mathbf{E}_P$: primary wave from a single reflection A (diffraction vector $\mathbf{g}_A$) and wavevector $\mathbf{k}_A = \mathbf{g}_A + \mathbf{k}_0$. Wave $\mathbf{E}_S$: secondary wave from reflection B (diffraction vector $\mathbf{g}_B$) coupled by reflection C (diffraction vector $\mathbf{g}_C = \mathbf{g}_A - \mathbf{g}_B$) and wavevector $\mathbf{k}_A = \mathbf{g}_C + \mathbf{k}_B$. The ϕ and χ rotation axes are aligned along $\mathbf{g}_A$ and the incident-beam direction, respectively.

synchrotron radiation (Morelhão & Avanci, 2001). The diffractometer allows the measurement of several azimuthal profiles with different values of $R_{max} = R(\phi_0)$, which is possible by varying the state of linear polarization. The data set composed of polarization-dependent ϕ-scans contains enough information to experimentally provide an accurate and reliable value of the triplet phase.

2. Three-axis goniometer

A systematic procedure to generate multiple X-ray waves in crystals is summarized as (i) choice of a primary reflection (reflection A); (ii) adjusting the incidence (ω) and detector (2θ) angles for exciting and monitoring the primary wave $\mathbf{E}_P$; (iii) alignment of the diffraction vector $\mathbf{g}_A$ with the ϕ rotation axis; and (iv) scanning the azimuthal axis (ϕ-scan) to generate the secondary wave $\mathbf{E}_S$. This procedure basically requires a goniometry of three circles, the 2θ, ω and ϕ circles, as shown in Fig. 2. It can easily be accomplished by a four-circle diffractometer, where the fourth circle is the Eulerian circle used to adjust the angle between the ω and ϕ axes. It is necessary for most common single-crystal diffraction experiments, but for n-BD experiments the ω and ϕ axes can be set orthogonal to each other and kept unchanged even during the crystal alignment. The final and precise positioning of the diffraction vector along the ϕ axis is carried out by the tilt arcs ω' and ω''. Since the incidence plane of the goniometer must rotate around the incident-beam direction for exploitation of the linear polarization of synchrotron radiation, the real necessity of designing a goniometer specifically for phase measurements is due to technical reasons. The extra weight of the Eulerian circle compromises the stability, alignment and cost of the equipment if it is to work in any inclined plane from the horizontal to the vertical. Then, the construction of a three-axis goniometer with orthogonal-built-in ω and ϕ axes significantly reduces the load capability required by the ω rotation stage as well as by the inclination table (χ-table), *i.e.* the table that rotates the whole goniometer around the incident-beam direction as shown in Fig. 3.

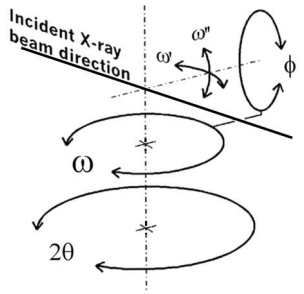

Figure 2
Three-axis goniometry for n-BD. The ω and ϕ axes are orthogonal, the ϕ axis lies in the incident plane, the plane of the ω and 2θ circles, and the direction of the ϕ axis rotates with ω. The ω' and ω'' arcs are used to align a diffraction vector to the direction of the ϕ axis.

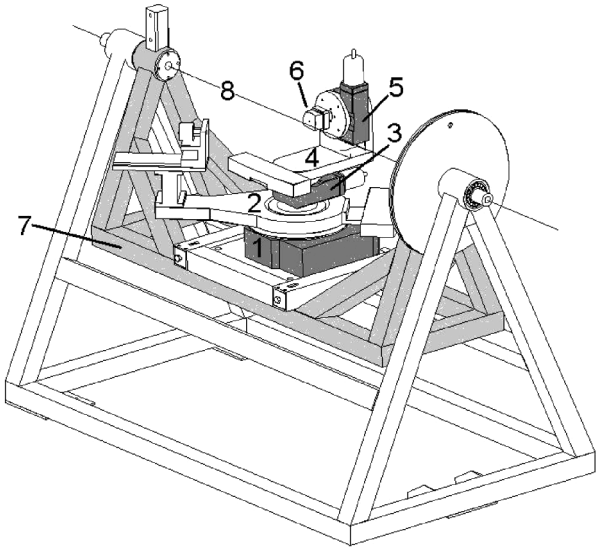

Figure 3
X-ray diffractometer for accurate triplet-phase determination. Parts 1 to 6 are components of the three-axis goniometer, 7 is the χ-table, and 8 shows the incidence-beam direction. 1, 3 and 5 are the 2θ, ω and ϕ rotation stages of the goniometer, respectively. 2 is the detector arm and 4 is attached to the ω axis. The goniometric head, 6, contains the ω' and ω'' arcs (Fig. 2) for precisely aligning the diffraction vector along the ϕ axis. In this figure, the incident plane is at the horizontal position.

3. Triplet phase determination with the diffractometer

The diffractometer in Fig. 3 is currently operating at the X-ray diffraction beamline (XRD-1) of the National Synchrotron Light Source (LNLS), Brazil. It is a bending-magnet beamline with a two-crystal Si(111) monochromator. Vertical and horizontal beam divergences are usually set to about 10" and 24", respectively. The very basic alignment procedure of the equipment consists of positioning the center of the goniometer, *i.e.* the intersection of the ω and ϕ axes, over the χ rotation axis of the table and aligning this axis along the incident-beam direction. The state of linear polarization of the synchrotron radiation with respect to the diffraction geometry is changed by the inclination of the χ-table. It is able to rotate the incidence plane of the goniometer at least from $\chi = -90^\circ$ to $+90^\circ$. $\chi = 0$ corresponds to the incident plane in the horizontal position (π polarization) and at $\chi = \pm 90^\circ$ it is vertical (σ polarization); the + and − signs denote the detector above and below the horizontal plane, respectively. For aligning the sample, a large goniometric head provides tilt arcs with a range of $\pm 25^\circ$. After setting the primary diffraction vector along the ϕ axis, it is also necessary to find a crystal reference direction for the azimuthal rotation. It allows the wavevector of the incident radiation to be described in the crystal's reciprocal space as a function of the ω and ϕ angles of the goniometer. Long ϕ-scans covering ranges of tens of degrees, also called Renninger scans (Renninger, 1937), sometimes have to be collected before being able to identify the position of the reference direction. In most cases the linear polarization breaks the intensity symmetry of n-BDs and only their positions obey the *symmetry mirrors*, as can be observed in Fig. 4.

To efficiently explore the linear polarization for measuring triplet phases, it is necessary to select the primary reflection and the X-ray wavelength to produce a scattering angle $2\theta_A$ near $\pi/2$. At this scattering geometry the strength of the primary wave is very tunable by the polarization direction, *i.e.* the inclination of the χ-table. The drastic effect of the σ and π polarizations in the profile of a *3*-BD when $2\theta_A = \pi/2$ is illustrated in the $\omega{:}\phi$ maps in Fig. 5. At $\chi = 0^\circ$ (π polarization) the primary reflection is forbidden by polarization, the contribution of the primary wave $|\mathbf{E}_P|^2$ is minimized and reference values are obtained for the intensity of the secondary wave $|\mathbf{E}_S|^2$. When the value of $|\mathbf{E}_S|^2$ at $\chi = 0^\circ$ is known, the value of R_{max} can be calculated for any polarization direction (see Fig. 6).

The extra degree of freedom given by the χ rotation of the incidence plane raises the following question: in what polarization should the triplet phase be measured? The intensity profiles have better sensitivity for measuring δ_T when the intensities of the waves are

almost the same, $R_{max} = |\mathbf{E}_S(\phi_0)|/|\mathbf{E}_P| \simeq 1$ (Weckert & Hümmer, 1997; Stetsko *et al.*, 2001, and references therein). In general there are two χ positions of the diffractometer where this happens, as shown in Fig. 6. The angle γ between the wavefields is different in each one of these positions, as already pointed out by Juretschke (1986). If the wavefields are orthogonal ($\gamma \simeq 90^\circ$), no phase information can be extracted from the intensity profiles, as demonstrated by the ϕ-scan at $\chi = -32^\circ$ in Fig. 7. Otherwise, any polarization where γ is near 0 or 180° can provide good data for extracting δ_T, as shown by other scans in Fig. 7.

For a general application of the diffractometer in triplet-phase determination, it is important to demonstrate that even in the cases where R_{max} cannot be directly measured, as for instance when $2\theta_A$ is different from $\pi/2$, the possibility of obtaining a polarization-dependent set of ϕ-scans solves the problem. Moreover, it also solves two other problems in phasing the *3*-BDs: (i) how to obtain the reliability of the determined value of δ_T, *i.e.* establishing the error bar, as in the above data set (Fig. 7) that provides an error in δ_T ($= -66.5^\circ$) of about $\pm 1.5^\circ$; and (ii) how to eliminate the systematic errors due to the *Aufhellung* effect (Wagner, 1923). In a few words, the *Aufhellung* is the reduction in the primary intensity due to the amount of energy taken out by the $\mathbf{k}_B$ beam (see Fig. 1). This effect becomes more significant as the intensity of the primary reflection increases with the polarization angle. The exact form of equation (1) is given in Appendix *A*, where the polarization coefficients, the adjustable parameter b' for empirical *Aufhellung* corrections, and the line profile function are shown explicitly. According to the notation used there, $R_{max} = R(v_S/v_P)$. Since R is independent of the polarization coefficients, hereafter the text will refer to R instead of to R_{max}. An example of the phasing procedure when R is unknown and *Aufhellung* occurs is provided by the data set in Fig. 8. By taking R and b' as global variables, the fit of each ϕ-scan is optimized by adjusting ξ and δ_T besides the peak position ϕ_0 and width w [see equation (6) for more details]. Then, the values of R and b' are also adjusted for producing a minimum deviation in δ_T, as shown in Fig. 9. In this case it provides an experimental value for δ_T of $37 \pm 2^\circ$.

For comparison, the theoretical values of the phase triplets for these *3*-BDs are provided here. In the GaSb crystal, by taking the origin of the unit cell at the Sb atoms, and its diagonal orientated

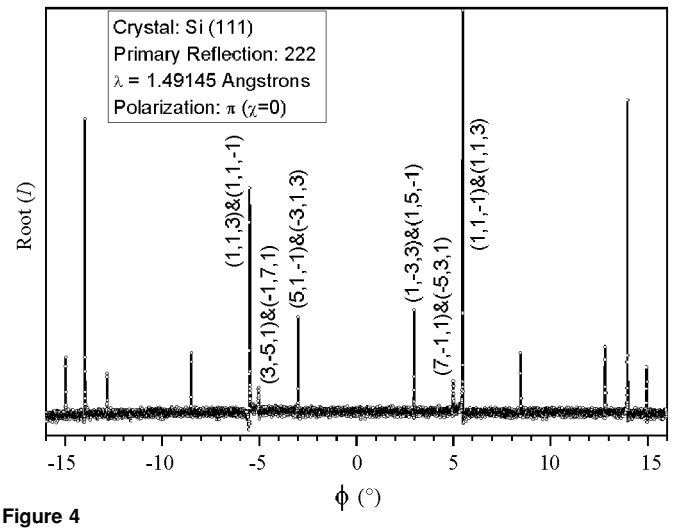

Figure 4
A Renninger scan (ϕ-scan) for locating the reference direction of the azimuthal rotation. The symmetry mirror position at $\phi = 0$ corresponds to the $[1\bar{1}0]$ crystal direction lying in the incidence plane of the goniometer. The indexes of the *B* and *C* reflections of some *3*-BDs are given. Step size: 0.005°.

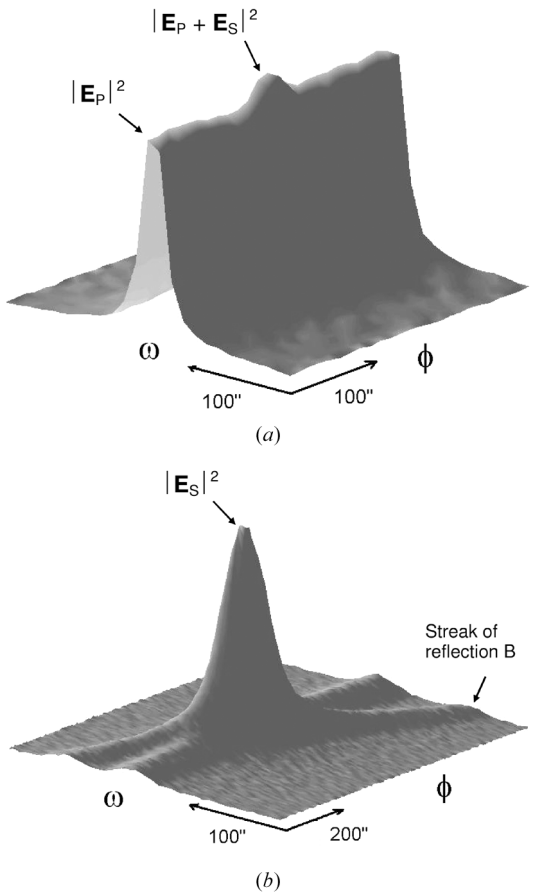

Figure 5
Two-dimensional intensity profiles (ω:ϕ maps) of a three-beam diffraction for (*a*) σ and (*b*) π polarizations. Primary wave $\mathbf{E}_P$ from reflection 006 (reflection *A*). Secondary wave $\mathbf{E}_S$ from reflections 113 and $\bar{1}\bar{1}3$ (*B* and *C* reflections). Crystal: GaSb (001). Wavelength: 1.4370 Å. Beam divergences: 9" (vertical) and 23.8" (horizontal). Mesh resolution: (*a*) 0.0032° and (*b*) 0.0016°.

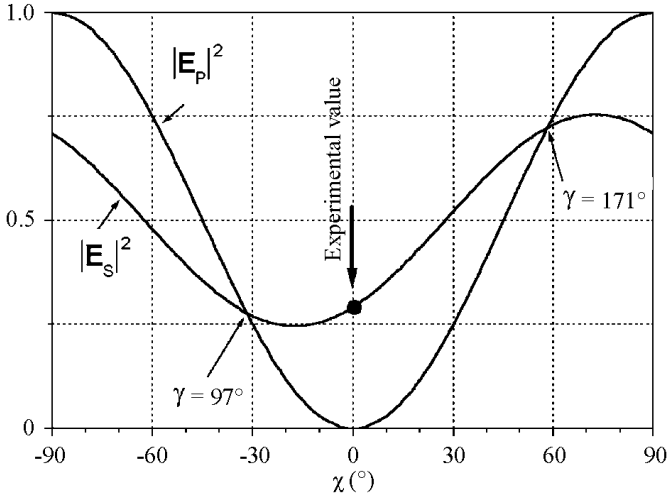

Figure 6
Relative intensities of the primary $|\mathbf{E}_P|^2$ and secondary $|\mathbf{E}_S|^2$ waves as a function of the polarization angle χ, the inclination of the χ-table. Reflection *A*: $\bar{2}26$. Reflections *B* and *C*: $\bar{3}13$ and 133. Crystal: GaSb (001). Wavelength: 1.2998 Å ($2\theta_A \simeq 90^\circ$). $I_P = 246\,265$ counts s^{-1} (at $\chi = 90^\circ$ and $\Delta\phi \neq 0$) and $I_S = 71\,814$ counts s^{-1} (at $\chi = 0^\circ$ and $\Delta\phi = 0$).

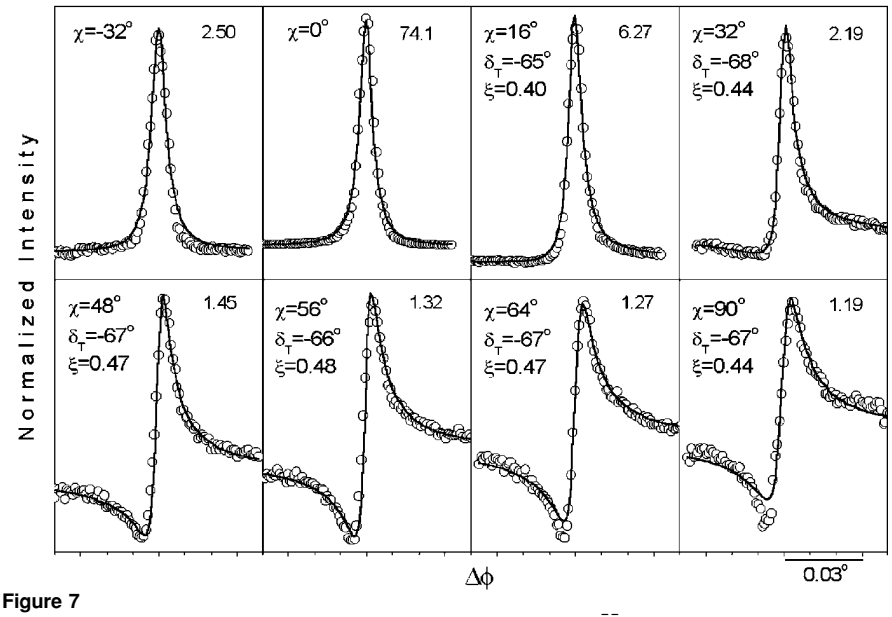

Figure 7
Experimental (open circles) and simulated (solid lines) ϕ-scans of the $\bar{3}\bar{1}3$ and 133 *3*-BD in GaSb crystal as a function of the polarization angle χ. Primary reflection: $\bar{2}26$. Simulated curves were generated using equation (2) (see Appendix *A*) for the 'out $\rightarrow$ in' position. The best-fit values of δ_T and ξ (for $R^2 = 1.334$ and $b' = 0$) are shown on the left-hand side of each scan. The number on the other side stands for the maximum intensity normalized by the base line, 1. Wavelength: 1.2998 Å ($2\theta_A \simeq 90°$). After Morelhão & Kycia (2002).

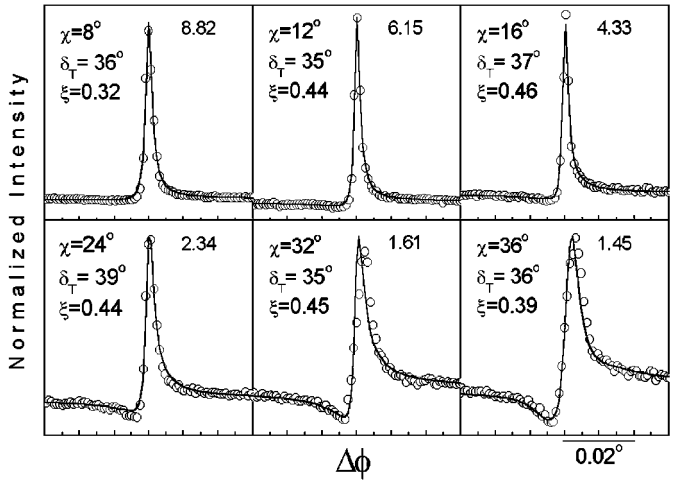

Figure 8
Experimental (open circles) and simulated (solid lines) ϕ-scans of the $33\bar{2}$ and $\bar{1}32$ *3*-BD in KDP (KH_2PO_4, potassium dihydrogen phosphate) crystal as a function of the polarization angle χ. Primary reflection: 260. Simulated curves were generated using equation (2) (Appendix *A*) for the 'out $\rightarrow$ in' position. The best-fit values of δ_T and ξ, for $R = 0.6515$ and $b' = 0.84$ [$R_{332} = 0.485$ and $R_{132} = 0.515$, see equation (3)], are shown on the left-hand side of each scan. The number on the other side stands for the maximum intensity normalized by the base line, 1. Wavelength: 1.65382 Å ($2\theta_A \simeq 90°$).

along the Sb—Ga bond, the phases of the $\bar{2}26$, $\bar{3}\bar{1}3$ and 133 reflections are $\delta_A = 0$, $\delta_B = -31°$ and $\delta_C = -31°$, respectively, which implies $\delta_T = -62°$. This was calculated for the atomic scattering factors, f^0_{Sb} and f^0_{Ga}, with a Debye–Waller *B* factor of 15 Å^2. If anomalous dispersion corrections, $f = f^0 + f' + if''$, are taken into account for a wavelength of 1.2992 Å ($f'_{Sb} = 0.067$, $f''_{Sb} = 4.383$, $f'_{Ga} = -2.194$ and $f''_{Ga} = 0.523$), the phase values become $\delta_A = 16.2°$, $\delta_B = -21.4°$, $\delta_C = -21.4°$ and $\delta_T = -59°$. Some corrections due to the formation of chemical bonds may also be considered. The cloud of charges due to shared electrons in the covalent bonds changes the average X-ray scattering around the atomic sites. One rough estimation of this effect is obtained by assuming an even contribution of the cloud to the scattering at either Sb and Ga sites. Since Sb atoms donate five electrons and Ga atoms donate three electrons to the cloud, the net charge, *i.e.* cloud/2 + core, around each site is better represented by Sb^{+1} and Ga^{-1}. In terms of the variation in the atomic scattering factors, it is represented by transferring one scattering charge unit from the Sb to the Ga atoms, $f_{Sb} \rightarrow f_{Sb} - 1$ and $f_{Ga} \rightarrow f_{Ga} + 1$, then the phase values become $\delta_A = 18.9°$, $\delta_B = -23.5°$, $\delta_C = -23.5°$ and $\delta_T = -65.9°$. In the case of the KDP crystal (KH_2PO_4), the phase triplet of the *3*-BD shown in Fig. 9 does not change its value by transferring one electron from K to P sites, and anomalous dispersion corrections are very small. With the origin of the unit cell at the P atoms, the phases of the 260, $33\bar{2}$ and $\bar{1}32$ reflections are $\delta_A = 0$, $\delta_B = 21.4°$ and $\delta_C = 13.2°$, respectively. Then, the phase triplet is $\delta_T = 34.6°$. Dispersion corrections provide $\delta_A = 6.3°$, $\delta_B = 24.8°$, $\delta_C = 16.9°$ and $\delta_T = 35.5°$ ($f'_P = 0.32$, $f''_P = 0.49$, $f'_K = 0.38$ and $f''_K = 1.2$ for $\lambda = 1.65382$ Å).

4. Discussion

Besides providing an experimental sense on the reliability of the measured phases, the polarization-dependent set of ϕ-scans is very important for developing or checking any theoretical description of the *3*-BD process in crystals. The standard second-order Born approximation, represented by equation (1) with $\xi = 1$, fails in reproducing all scans in the set with the same triplet-phase values, after adjusting the *R*-value to reproduce the curve at $\chi = 0$. As the

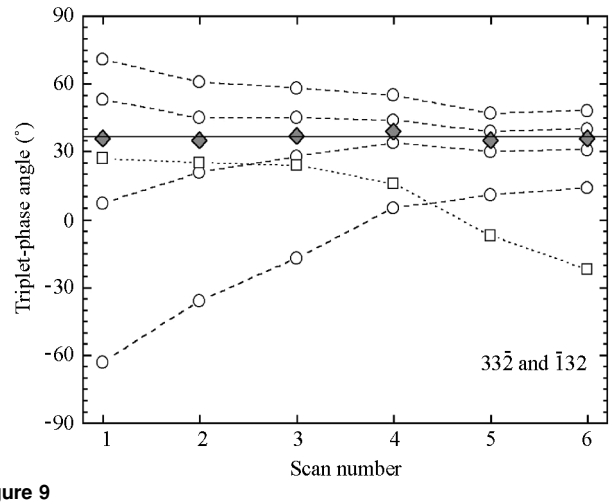

Figure 9
Comparison of the triplet-phase angles obtained from fitting the ϕ-scans in Fig. 8 with different values of *R* and b'. The minimum deviation in the triplet-phase values is obtained for $R = 0.6515$ and $b' = 0.84$ (shaded diamonds). The horizontal solid line shows the theoretical value, $\delta_T = 35.6°$. The open circles show changes of −20%, −5%, +5% and +20% in *R*, from top to bottom, respectively. The open squares show the systematic error if *Aufhellung* is neglected ($b' = 0$). The scan number refers to the ϕ-scans in Fig. 8 as ordered.

polarization angle increases, the asymmetries of the profiles due to the interference of the primary and secondary waves are very much enhanced in theory, *i.e.* in the simulated curves, than observed in the experimental curves. On the framework of the second-order approximation, this fact suggests that not all of the power (intensity) assigned to the secondary wave at $\chi = 0$ is interfering with the primary wave as it is excited at higher χ angles, as for instance if crystalline defects were present in the diffracting crystal volume. For this reason, the ξ parameter was included in equation (1) to reduce the contribution of the interference term. Does $\xi < 1$ mean that the diffracted beams have a partial capability to interfere? Or is it just a consequence of the incompleteness of this theoretical approach? The true answer to such questions will be the subject of future works, but what can certainly be said at this moment is that, by assuming $\xi = 1$ in equation (1), very significant systematic errors are generated in the experimental values of the triplet phases as shown elsewhere (Morelhão & Kycia, 2002).

There are very accurate theoretical descriptions of the *3*-BD process in perfect crystals, as provided by the *n*-beam dynamical theory (Colella, 1974; Weckert & Hümmer, 1997) or the expanded distorted-wave Born approximation (Shen, 1999). When such theories are applied in phase determination, they implicitly assume that no crystalline defects are visible in the diffracting volume by any of the three reflections (A, B or C) of the respective *3*-BD case. The data-collection procedure proposed here is able to not only check the validity of such an assumption but also to figure out the price paid for it, *i.e.* the systematic error that it generates. Moreover, new theoretical approaches can be proposed for describing the diffraction process when particular or several types of defects are present in the crystals. The approach in Appendix *A* is limited to samples where the profile functions of the scattered intensities from the hypothetical crystal defects as well as of the *Aufhellung* effect are the same function used to simulate the *3*-BD profile in the perfect lattice, *i.e.* $|f(\phi)|$. Whatever the proposed approach is, it has to fit not only one ϕ-scan but also a polarization-dependent set of ϕ-scans, as well as to provide the same triplet phase for all polarizations, at least for those polarizations where the *Aufhellung* is not dominant, as shown for the data set in Fig. 8.

In both polarization-dependent data sets, Figs. 7 and 8, the ξ parameter is observed to vary as a function of the polarization angle χ. There are several hypotheses that could be considered as plausible sources of such variation: contamination of the incident beam due to some amount of non-linearly polarized radiation (further discussion on this hypothesis is provided at the end of Appendix *A*); translation of the beam spot on samples with non-uniform density of crystalline defects; or even the χ-rotation of the incidence plane with respect to the X-ray optics, which affect how the primary and double-bounce reflections interact with both the vertical energy fan from the monochromator and the beam divergences. All these hypotheses will require further investigation, for which the instrumental degree of freedom for carrying out ϕ-scans at several polarization angles is essential. Since there are several reasons for such variation, ξ cannot be taken as a global variable for fitting the data set. It's value has to be adjusted along with δ_T for each ϕ-scan.

5. Conclusion

For accurate determination of the invariant phase triplets, exploitation of linearly polarized synchrotron radiation is very important. It requires an X-ray diffractometer similar to the one described in this article, or a more expensive one, to allow data collection for composing a polarization-dependent set of ϕ-scans. Otherwise, insertion devices capable of rotating the linear polarization direction have to be developed to operate in the X-ray energy range used in crystallography. Since the polarization-dependent data set breaks the degeneracy of the azimuthal profiles due to partial interference of the diffracted beams, the data set can provide the necessary experimental evidence for guiding the development of new theoretical approaches for the *three*-beam diffraction phenomenon, *i.e.* approaches capable of phasing real non-perfect crystals, where at least a minimum of asymmetry can still be observed in the azimuthal profiles.

APPENDIX *A*
Modified second-order Born approximation of the three-beam diffraction

The complete parametric form (Morelhão & Kycia, 2002) of the equation used to simulate the profiles presented in this article is

$$I(\phi) = v_P^2\Big[1 - b\big|f(\phi)\big|^2\Big] + R^2\big|f(\phi)\big|^2 v_S^2 + 2\xi R\big|f(\phi)\big|\mathbf{v}_P \cdot \mathbf{v}_S \cos(\Omega + \delta_T). \quad (2)$$

The primary and secondary waves were normalized by the amplitude reflectivity of the primary reflection, $\mathbf{E}_\mathrm{P} = \mathbf{v}_\mathrm{P}$ and $\mathbf{E}_\mathrm{S} = Rf(\phi)\exp(i\delta_T)\mathbf{v}_\mathrm{S}$, where

$$f(\phi) = \pm w/\big[2(\phi - \phi_0) \mp iw\big] \quad (3)$$

is the line profile function used to describe the excitation of the secondary wave with the ϕ rotation. The + and − signs in the numerator denote the cases where the diffraction vector $\mathbf{g}_B$ moves from the outside to the inside, 'out → in', of the Ewald sphere and *vice versa*, 'in → out', respectively. The Lorentzian width w determines the range of the secondary field from its maximum at ϕ_0. ξ is defined in §1, and

$$b = b'(R_B v_B^2 + R_C v_C^2), \quad (4)$$

where R_G is estimated as $|F_G|^2/(|F_B|^2 + |F_C|^2)$ and F_G is the theoretical structure factor of reflection G (= B or C). The polarization coefficients depend on the direction of the diffracted beams, $\mathbf{k}_{A,B} = \mathbf{g}_{A,B} + \mathbf{k}_0$, as well as on the polarization direction, $\hat{\mathbf{e}}$, and were calculated according to

$$\begin{aligned}
\mathbf{v}_\mathrm{P} &= \hat{k}_A \times (\hat{k}_A \times \hat{e}),\\
\mathbf{v}_\mathrm{S} &= \hat{k}_A \times \{\hat{k}_A \times [\hat{k}_B \times (\hat{k}_B \times \hat{e})]\},\\
\mathbf{v}_B &= \hat{k}_B \times (\hat{k}_B \times \hat{e}),\\
\mathbf{v}_C &= \hat{k}_B \times \{\hat{k}_B \times [\hat{k}_A \times (\hat{k}_A \times \hat{e})]\}.
\end{aligned} \quad (5)$$

The polarization direction with respect to the rotation angle χ of the incidence plane of the diffractometer has been written as $\hat{e} = \sin(\chi)\hat{\sigma} - \cos(\chi)\hat{\pi}$, where $\hat{\sigma} = \hat{k}_0 \times \hat{k}_A / \sin 2\theta_A$ and $\hat{\pi} = \hat{\sigma} \times \hat{k}_0$.

To compare the simulated and experimental ϕ-scans, the error function

$$\mathbf{E}(\mathbf{p}) = [1/(N-1)]\sum_{n=1}^{N}\big|I(\phi_n, \mathbf{p}) - I_\mathrm{EXP}(\phi_n)\big| \quad (6)$$

has been used, where $\mathbf{p} = [\phi_0, w, R, b', \xi, \delta_\mathrm{T}]$ is the parameter vector of the adjustable parameters and N is the total number of data points in the scan.

A1. Non-linearly polarized radiation

A small amount of circular/elliptically polarized radiation can exist in the incident beam. It provides extra contributions to both the $\mathbf{E}_\mathrm{P}$

and $\mathbf{E}_S$ waves. The primary wavefield is always σ polarized when scattered at $\pi/2$ from the incident-beam direction. The direction of the secondary wavefield varies with χ, but only its σ component participates in the interference term, which is properly taken into account by the dot product $\mathbf{v}_P \cdot \mathbf{v}_S$ in equation (2). Circular/elliptically polarized radiation sent through the double-bounce reflection, $B + C$, provides an extra σ component, $\boldsymbol{\sigma}_{\rm extra}$, in the interference term. The dependence of these contributions on the polarization angle χ is different to that predicted by equation (5). It produces variations in ξ to compensate this extra σ component. The interference term, $I_\sim$, of equation (2) is sensitive to the contamination of non-linearly polarized radiation according to

$$I_\sim = 2R\left|f\right|v_P\left(v_S\xi_0\cos\gamma + \Delta u\right)\cos(\Omega + \delta_T),$$

where $\mathbf{v}_P \cdot \mathbf{v}_S = \cos\gamma$ and $\mathbf{v}_P \cdot \boldsymbol{\sigma}_{\rm extra} = \Delta u$. Since ξ, instead of ξ_0, is the fitting parameter, its dependence with the polarization angle is given by $\xi = \xi_0 + \Delta u/v_S \cos\gamma$.

The author would like to acknowledge the LNLS for constructing the χ-table, in particular A. R. D. Rodrigues, R. T. Neuenschwander and S. Kycia. This work was supported by the Brazilian founding agencies FAPESP (for acquisition of the three-axis goniometer, Grant No. 97/13757-8) and CNPq (Proc. No. 301617/95-3). Thanks are due to C. M. R. Remédios for the KDP samples.

References

Chang, S. L. (1982). *Phys. Rev. Lett.* **48**, 163–166.
Chang, S. L. & Tang, M. T. (1988). *Acta Cryst.* A**44**, 1065–1069.
Colella, R. (1974). *Acta Cryst.* A**30**, 413–423.
Hart, M. & Lang, A. R. (1961). *Phys. Rev. Lett.* **7**, 120–121.
Helliwell, J. R. (2002). *J. Synchrotron Rad.* **9**, 1–8.
Juretschke, H. J. (1986). *Phys. Status Solidi B*, **135**, 455–459.
Morelhão, S. L. & Avanci, L. H. (2001). *Acta Cryst.* A**57**, 192–196.
Morelhão, S. L. & Kycia, S. (2002). *Phys. Rev. Lett.* **89**(1), 015501.
Post, B. (1977). *Phys. Rev. Lett.* **39**, 760–763.
Renninger, M. (1937). *Z. Kristallogr.* **97**, 107–121.
Shen, Q. (1999). *Phys. Rev. B*, **59**, 11109–11112.
Shen, Q. & Colella, R. (1987). *Nature (London)*, **329**, 232–233.
Shen, Q. & Colella, R. (1988). *Acta Cryst.* A**44**, 17–20.
Stetsko, Yu. P., Juretschke, H. J., Huang, Y.-S., Lee, Y.-R., Lin, T.-C. & Chang, S.-L. (2001). *Acta Cryst.* A**57**, 359–367.
Wagner, E. (1923). *Phys. Z.* **21**, 94–99.
Weckert, E. & Hümmer, K. (1997). *Acta Cryst.* A**53**, 108–143.

 Received 3 July 2002 • Accepted 18 February 2003